

Article

# Effect of the Number of Leaves in Submerged Aquatic Plants on Stream Flow Dynamics

Peiru Yan <sup>1</sup>, Yu Tian <sup>2,\*</sup>, Xiaohui Lei <sup>2</sup>, Qiang Fu <sup>3,4,5</sup>, Tianxiao Li <sup>3,4,5</sup> and Jiahong Li <sup>1</sup>

<sup>1</sup> School of Civil Engineering, Tianjin University, Tianjin 300072, China

<sup>2</sup> State Key Laboratory of Simulation and Regulation of Water Cycle in River Basin, China Institute of Water Resources and Hydropower Research, Beijing 100038, China

<sup>3</sup> School of Water Conservancy and Civil Engineering, Northeast Agricultural University, Harbin 150030, China

<sup>4</sup> Key Laboratory of Effective Utilization of Agricultural Water Resources of Ministry of Agriculture, Northeast Agricultural University, Harbin 150030, China

<sup>5</sup> Heilongjiang Provincial Key Laboratory of Water Resources and Water Conservancy Engineering in Cold Region, Northeast Agricultural University, Harbin 150030, China

\* Correspondence: sweetrain511@163.com

Received: 12 June 2019; Accepted: 9 July 2019; Published: 13 July 2019



**Abstract:** The main purpose of this study is to investigate the effects of aquatic plants with no leaves (L0), 4 leaves (L4), 8 leaves (L8), and 12 leaves (L12) on the mean streamwise velocity, turbulence structure, and Manning's roughness coefficient. The results show that the resistance of submerged aquatic plants to flow velocity is discontinuous between the lower aquatic plant layer and the upper free water layer. This leads to the difference of flow velocity between the upper and lower layers. An increase of the number of leaves leads to an increase in the flow velocity gradient in the upper non-vegetation area and a decrease in the flow velocity in the lower vegetation area. In addition, aquatic plants induce a momentum exchange near the top of the plant and increase the Reynold's stress and turbulent kinetic energy. However, because of the inhibition of leaf area on the momentum exchange, the Reynold's stress and turbulent kinetic energy increase first and then decrease with the increase in the number of leaves. Quadrant analysis shows that ejection and sweep play a dominant role in momentum exchange. Aquatic plants can also increase the Reynold's stress by increasing the ejection and sweep. The Manning's roughness coefficient increases with the increasing number of leaves.

**Keywords:** submerged flexible vegetation; flow velocity; Reynold's stress; turbulent kinetic energy; Manning's roughness coefficient

## 1. Introduction

Aquatic plants are an important component of river ecosystems. They can not only affect water chemical and physical parameters, but, more importantly, they can also change flow velocity and momentum exchange, and consequently affect the transport of pollutants and sediments in rivers [1–5].

The acoustic Doppler velocimeter (ADV) has been widely used in both laboratory and field settings for the measurement of flow velocity [1,3,6]. ADV is based on based on the Doppler effect and can accurately measure the mean velocities and turbulent statistical parameters [7], especially the flow characteristics under the influence of aquatic plants [1,3].

The effect of aquatic plants on the flow characteristics is closely related to the density, structure, foliage surface area, height, biomass, and arrangement of aquatic plants [8,9]. Zhang et al. [10] found that vegetation could significantly change the vertical flow velocity profile. Huai et al. [11]

developed an analytical model for predicting the vertical distribution of mean streamwise velocity with double-layered rigid vegetation. Han et al. [12] predicted the vertical streamwise velocity profile in the presence of floating vegetation using a two-power law expression. Tang et al. [13] investigated the drag coefficients and their applications in the modelling of turbulent flow with submerged vegetation, and found that the model with the drag coefficient for an isolated cylinder and the local drag coefficient could better predict velocity distribution than that with the bulk drag coefficient. Wilson et al. [14] found that the frond foliage induced larger drag forces and inhibited the momentum exchange. Li et al. [15] found that the maximum turbulence intensity and Reynold's stress of water flow increased with the increase of plant height. Dodds and Biggs [16] developed a model unifying attenuation by periphyton and macrophytes using the biomass density as the independent variable, which explained 80% of the variation in attenuation. In addition, the conditions of the river bed and the external environment also have some impact on the flow [17–19]. Devi and Kumar [18] investigated the characteristics of turbulent flow in a vegetative channel with seepage and found that seepage increased the maximum Reynold's stress and turbulence intensity. Wang et al. [20] found that the spatial variation in drag coefficient through the vegetated patch exhibited either a monotonic decline during rain or a non-monotonic 'hump' shape without rain with increasing longitudinal distance in the vegetated section.

However, previous research has not considered the variation of flow characteristics with the number of leaves. Given the substantial difference in the growth of aquatic plants in different seasons, it is important to study the effects of aquatic plants with different numbers of leaves on river flow characteristics in order to accurately predict flow velocity and pollutant diffusion. In response to this need, the main purpose of this study is to study the effects of aquatic plants with different numbers of leaves on the mean streamwise velocity, turbulence structure, and Manning's roughness coefficient.

## 2. Materials and Methods

### 2.1. Experimental Equipment and Procedure

The experimental equipment used in this study includes two pumps, a stilling basin, an underground reservoir, a rectangular tank, and an adjustable tail gate. The open-channel flume is 29 m long, 0.6 m wide, and 0.7 m high, and made of glass, which is schematically shown in Figure 1. An energy dissipation grate is installed at the inlet of the flume to ensure a steady flow of water into the flume, and an adjustable tail gate is installed at the tail to control the water level.

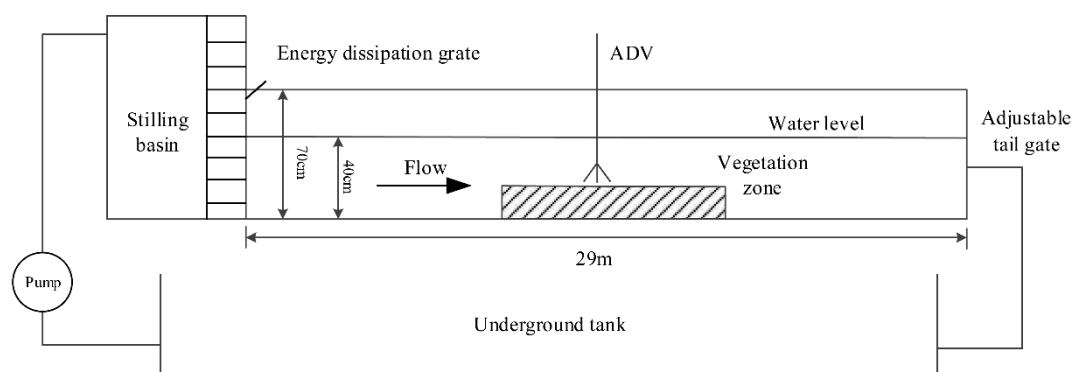


**Figure 1.** General layout of the open channel flume. ADV—acoustic Doppler velocimeter.

Flexible aquatic plants are simulated using plastic materials, where the plant height is 20 cm; the leaf length is 17 cm; the leaf is arc-shaped, which is narrower at both ends and wider at the middle; the top width is 0.5 mm; the bottom width is 2 mm; and the middle width is about 1 cm (Figure 2).



Figure 2. The layout and shape of plants.

In this experiment, the flow rate was set to 0.06 m<sup>3</sup>/s and the water level was set to 0.4 m. Aquatic plants were arranged in a staggered pattern over a length of 7 m. There were a total of seven measurement sections with 11 points spaced 3 cm apart in each section (Figure 3). The velocity was measured using an acoustic Doppler velocimeter (ADV; Vectrino, Nortek, Norway) with a frequency of 20 Hz for 120 s. The data for each point were composed of 2400 samples, from which the average velocity was calculated. Note that the velocity 5 cm below the water surface and 5 cm above the flume bottom could not be measured because of the limitation of ADV. In order to ensure high measurement accuracy, glass sand with a diameter of 10 microns was added, and the accelerated threshold method was used to post-process the data [18]. Submerged aquatic plants often have 4–12 leaves [21], and the average number of leaves is 7 in the study of Zhang and Lai [22]. Therefore, the effects of aquatic plants with no leaves (L0), 4 leaves (L4), 8 leaves (L8), and 12 leaves (L12) on the flow characteristics were investigated in this study.

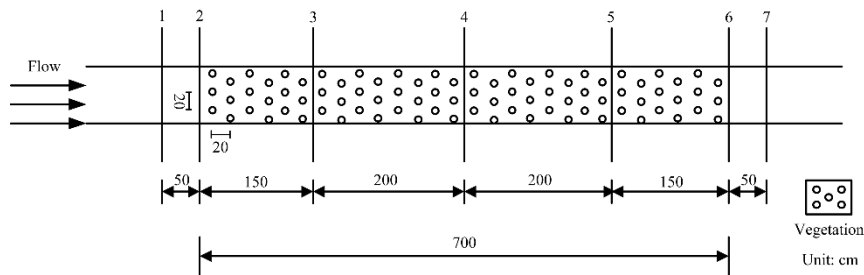


Figure 3. Locations of measurement sections in the flume.

## 2.2. Methods

### 2.2.1. Mean Velocity, Reynold’s Stress, and Turbulent Kinetic Energy

The mean velocity  $u$ , Reynold’s stress  $\tau_{xz}$ , and turbulent flow energy  $k$  are three important parameters characterizing the flow structure:

$$u = (1/m) \times \sum_{i=1}^m u_i, \tag{1}$$

$$u' = u_i - u, \tag{2}$$

$$\tau_{xz} = \overline{u'v'}, \tag{3}$$

$$u_{rms} = \sqrt{\overline{u'^2}}, \tag{4}$$

$$k = 0.5 \times (u_{rms}^2 + v_{rms}^2 + w_{rms}^2), \tag{5}$$

where  $u$  is the mean streamwise velocity,  $u_i$  is the instantaneous streamwise velocity,  $u'$  is the fluctuation of the streamwise velocity,  $v'$  is the fluctuation of the vertical velocity,  $\tau_{xy}$  is the Reynold’s stress,  $u_{rms}$  is

the root mean square of the streamwise velocity,  $v_{rms}$  is the root mean square of the vertical velocity,  $w_{rms}$  is the root mean square of the spanwise velocity, and  $k$  is the turbulent kinetic energy.

### 2.2.2. Logarithmic Distribution Law

The mean streamwise velocity profile can be divided into two layers according to the vegetation height: lower aquatic plant layer and upper free water layer. This division is largely consistent with previous studies [23–25]. For instance, Huai et al. [23] also divided the velocity profile into two layers, including the upper free water layer and the lower plant layer, according to the bending height of plants. Li et al. [25] divided the velocity profile into three layers, including the upper free water layer, the middle canopy layer, and the lower sheath layer, according to the position of canopy top and sheath and leaf. In this study, the mean streamwise velocity profile is divided into two layers according to the vegetation height because the stem is very short (about 2 cm). However, the mean streamwise velocity profile in the upper free water layer is similar to that in the non-vegetation area, which obeys the logarithmic distribution law [1,25]. This may be attributed to the formation of a new “soft river bed” at the top of the plant. In order to better understand the mean streamwise velocity profile in the upper free water layer, the following formula is used to describe the mean streamwise velocity profile at different positions [1].

$$u(z)/u_0 = a + b \times C(z/h), \quad (6)$$

where  $z$  is the vertical coordinate;  $u(z)$  is the mean streamwise velocity at  $z$ ;  $u_0$  is the mean streamwise velocity of a fully developed flow;  $h$  is the plant height;  $C$  is a function of  $z/h$ , which can be represented by different log equations ( $\ln(x)$ ,  $\ln(x)/x^2$ ,  $\ln(x)/x^{2.5}$ , and  $\ln(x)/x^3$ , where  $x = z/h$ ); and  $a$  and  $b$  are constants.

### 2.2.3. Manning’s Roughness Coefficient

The Manning’s roughness coefficient is calculated from the following equation:

$$n = 1/u \times R_h^{2/3} S^{1/2}, \quad (7)$$

where  $n$  is the Manning’s roughness coefficient,  $R_h$  is the hydraulic radius, and  $S$  is the energy slope. In this study, the Manning’s roughness coefficient proposed by Noarayanan et al. [26] is used, which can be calculated from the following equation:

$$n_{veg} = \left\{ (1/u_{(veg+non)}) \times (R_h^{2/3} \times S_{(veg+non)}^{1/2}) \right\} - \left\{ (1/u_{(non)}) \times (R_h^{2/3} \times S_{(non)}^{1/2}) \right\}, \quad (8)$$

$$S_{(veg+non)} = H_{f(veg+non)} / L, \quad (9)$$

$$S_{(non)} = H_{f(non)} / L, \quad (10)$$

$$H_{f(veg+non)} = \left\{ \left( (u_{u(veg+non)}^2 - u_{d(veg+non)}^2) / 2g \right) + (h_{u(veg+non)} - h_{d(veg+non)}) \right\}, \quad (11)$$

$$H_{f(non)} = \left\{ \left( (u_{u(non)}^2 - u_{d(non)}^2) / 2g \right) + (h_{u(non)} - h_{d(non)}) \right\}, \quad (12)$$

where  $n_{veg}$  is the Manning’s roughness coefficient of the plant,  $u_{u(veg+non)}$  is the upstream velocity measured with vegetation,  $u_{u(non)}$  is the upstream velocity measured without vegetation,  $h_{u(veg+non)}$  is the depth of flow at the upstream of the vegetation,  $h_{u(non)}$  is the depth of flow at the upstream without vegetation,  $u_{d(veg+non)}$  is the downstream velocity measured with vegetation,  $u_{d(non)}$  is the downstream velocity measured without vegetation,  $h_{d(veg+non)}$  is the depth of flow at the downstream of the vegetation,  $h_{d(non)}$  is the depth of flow at the downstream without vegetation,  $S_{(veg+non)}$  is the energy slope with vegetation,  $S_{(non)}$  is the energy slope without vegetation,  $H_{f(veg+non)}$  is the water head loss with vegetation,  $H_{f(non)}$  is the water head loss without vegetation, and  $L$  is the length of vegetation area. The data were analyzed using Excel 2016, SPSS 22, and Matlab 2010.

### 3. Results and Discussion

#### 3.1. Mean Streamwise Velocity

Flow velocity can affect the water-carrying capacity of rivers and the erosion at the bottom of rivers. Considering that the existence of vegetation may change the distribution of flow velocity, the mean streamwise velocity profile under L0, L4, L8, and L12 is shown in Figure 4.

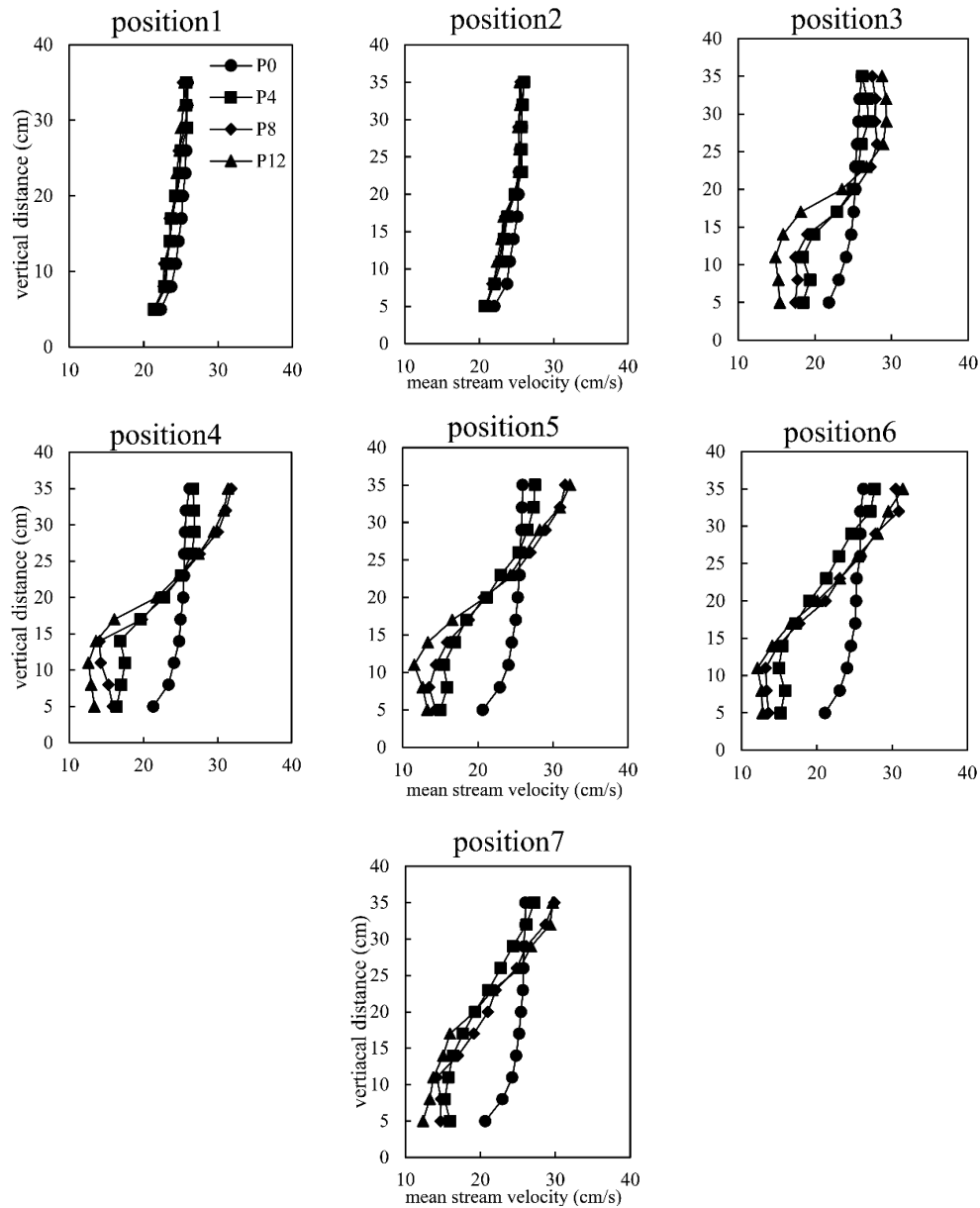


Figure 4. The mean streamwise velocity profile under different leaf numbers.

Figure 4 shows that there is only a small difference in flow velocity between position 1 and 2, which conforms to the traditional velocity distribution law. However, it is noted that the velocity in the upper layer gradually follows the logarithmic distribution law, while that in the lower layer decreases because of the obstacle of plants. The velocity distribution in the presence of plants differs greatly from that without plants.

In order to better understand the mean streamwise velocity profile in the upper free water layer, the parameters  $a$  and  $b$  and the logarithmic equation  $C$  were calculated from Equation (6).

The parameters  $a$  and  $b$  and the logarithmic equation  $C$  at different positions under L0, L4, L8, and L12 are listed in Table 1. It shows that the fitting is good at all positions ( $R^2 > 0.96$ ) except that at position 3 of P4. The parameter  $b$  and the logarithmic equation  $C$  represent different velocity gradients ( $\Delta(u/u_0)/\Delta(z/hp)$ ). The velocity gradient of each equation is  $\ln(x) > \ln(x)/x^2 > \ln(x)/x^{2.5} > \ln(x)/x^3$ . In the same equation, the velocity gradient increases with the increase of parameter  $b$ . It can be seen from Table 1 that the velocity gradient at all positions, except that at position 3, increases with the increase of the number of leaves. Li et al. [25] also found that the velocity gradient in the upper non-vegetation area increased as the plant density increased. This could be attributed to the increase in the number of leaves of underlying plants. An increase in the number of leaves can also increase the shear stress between the top of the plant and the flow and, consequently, an increase in the flow velocity gradient that is proportional to the shear stress. At position 3, the distance between the measurement position and the entrance of the vegetation area is too short to enable plants to have an effect on the flow.

**Table 1.** Parameters  $a$  and  $b$  and logarithmic equation  $C$  under different cases.

Cases	Function	Position			
		3	4	5	6
P4	$a$	0.9931	0.9113	0.5161	0.7574
	$b$	0.867	2.069	0.5448	0.6418
	$C(x)$	$\ln(x)/x^2$	$\ln(x)/x^2$	$\ln(x)$	$\ln(x)$
	$R^2$	0.8088	0.9887	0.9808	0.9898
P8	$a$	1.01	0.9104	0.8606	0.8378
	$b$	2.041	0.702	0.7775	0.7415
	$C(x)$	$\ln(x)/x^3$	$\ln(x)$	$\ln(x)$	$\ln(x)$
	$R^2$	0.9865	0.9809	0.9801	0.9673
P12	$a$	0.934	0.8907	0.8464	0.8068
	$b$	3.644	0.712	0.8003	0.8094
	$C(x)$	$\ln(x)/x^{2.5}$	$\ln(x)$	$\ln(x)$	$\ln(x)$
	$R^2$	0.9848	0.9776	0.9951	0.9976

Note:  $x = z/h$ .

In the lower aquatic plant layer, because the leaf of simulated aquatic plants is narrow at both ends and wide at the middle, the average velocity decreases first and then increases. The presence of aquatic plants also leads to a decrease in the area of flow through the lower vegetation area, and thus the mean flow velocity under L4, L8, and L12 is 20.60%, 23.46%, and 29.53% lower than that under L0, respectively. Also, the higher the number of leaves, the lower the mean flow velocity. Li et al. [25] found that the mean flow velocity in the lower vegetation area (middle canopy area and lower sheath area) decreased with the increase of plant density, which was related to the water-blocking area of plants. In this study, an increase in the number of leaves could also increase the water-blocking area of plants. Devi and Kumar [18] found that the mean velocity in the lower vegetation zone was still reduced under seepage conditions, but seepage would reduce the water-blocking effect of plants and increase the mean velocity. Clearly, aquatic plants can reduce the erosion of the river bed through slowing down the flow at the river bottom. In addition, the uncertainty is also important for experiments [27,28], and it was calculated using the Taylor Series Method in Table 2. As shown in Table 2, the uncertainty ranges from 0.3 to 1.5 cm/s, which is mainly caused by the fluctuation of flow [29].

**Table 2.** The mean velocity ratio under different cases.

Cases	Velocity cm/s	Position						
		1	2	3	4	5	6	7
P0	$u_n$	25.7 <sup>a</sup> ±0.5	25.6 <sup>a</sup> ±0.5	26.0 <sup>a,b</sup> ±0.4	25.7 <sup>a,b</sup> ±0.4	25.7 <sup>a,b</sup> ±0.3	25.7 <sup>a</sup> ±0.3	25.8 <sup>a</sup> ±0.3
	$u_v$	24.2 <sup>b</sup> ±0.7	24.1 <sup>b</sup> ±0.7	24.0 <sup>a</sup> ±0.6	24.0 <sup>b</sup> ±0.7	23.7 <sup>b</sup> ±0.6	23.8 <sup>a</sup> ±0.7	23.9 <sup>a</sup> ±0.7
	$u_n/u_v$	1.06	1.06	1.07	1.07	1.08	1.08	1.08
P4	$u_n$	25.2 <sup>a</sup> ±0.5	25.6 <sup>a</sup> ±0.4	26.1 <sup>b</sup> ±0.4	25.8 <sup>a,b</sup> ±0.6	25.2 <sup>a,b</sup> ±0.7	23.8 <sup>a</sup> ±0.8	23.5 <sup>a</sup> ±0.9
	$u_v$	23.1 <sup>c</sup> ±0.7	22.9 <sup>c</sup> ±0.6	20.6 <sup>c</sup> ±0.5	18.1 <sup>c</sup> ±0.6	17.2 <sup>c</sup> ±0.7	16.2 <sup>b</sup> ±0.6	16.7 <sup>b</sup> ±0.7
	$u_n/u_v$	1.09	1.12	1.27	1.43	1.47	1.46	1.40
P8	$u_n$	25.1 <sup>a</sup> ±0.5	25.4 <sup>a</sup> ±0.5	27.3 <sup>b</sup> ±0.5	28.0 <sup>a</sup> ±1.3	27.4 <sup>a</sup> ±1.2	26.5 <sup>a</sup> ±1.3	25.4 <sup>a</sup> ±1.3
	$u_v$	23.1 <sup>c</sup> ±0.7	22.8 <sup>c</sup> ±0.7	19.9 <sup>c</sup> ±0.7	16.9 <sup>c,d</sup> ±1.0	16.3 <sup>c</sup> ±1.1	15.6 <sup>b</sup> ±1.1	16.8 <sup>b</sup> ±1.1
	$u_n/u_v$	1.09	1.11	1.37	1.66	1.69	1.70	1.51
P12	$u_n$	24.9 <sup>a</sup> ±0.5	25.2 <sup>a</sup> ±0.5	27.7 <sup>b</sup> ±0.7	27.5 <sup>a</sup> ±0.9	27.2 <sup>a</sup> ±1.1	26.3 <sup>a</sup> ±1.5	25.3 <sup>a</sup> ±1.4
	$u_v$	23.2 <sup>c</sup> ±0.6	22.7 <sup>c</sup> ±0.7	17.1 <sup>d</sup> ±0.7	15.1 <sup>d</sup> ±0.8	14.7 <sup>c</sup> ±0.9	14.7 <sup>b</sup> ±1.0	14.9 <sup>b</sup> ±1.1
	$u_n/u_v$	1.07	1.11	1.62	1.83	1.84	1.79	1.70

Note: values within a column followed by the same letter are not significantly different (LSD),  $p < 0.05$ .

Clearly, the presence of aquatic plants results in a significant difference in velocity between the upper and lower layers and changes the ratio of flow velocity between the upper and lower layers. The mean flow velocity in the upper layer of L0 is slightly higher than that in the lower layer with a ratio of about 1.07; while the ratios of L4, L8, and L12 are around 1.11 at the entrance of the vegetation area (position 2). However, the ratios become stable with the development of flow, but there is a slight difference in the location at which a stable ratio is obtained. The stable ratio of L8 and L12 is observed at position 4, while that of L4 is observed at position 5. When the mean flow velocity ratio is stable (position 5), the mean flow velocity ratios of L4, L8, and L12 are 35.98%, 55.26%, and 70.58% higher than that of L0, respectively.

Flow will be resisted by aquatic plants in the vegetation area, resulting in changes of flow force. The ratio of the mean velocity between upper and lower layers is used to determine whether the flow has reached equilibrium. When the ratio is stable, the flow is considered to reach equilibrium. Table 2 shows that the flow of L8 to L12 reaches equilibrium at position 4, while that of L4 reaches equilibrium at position 5. Table 1 shows that the upper mean velocity distributions of L4, L8, and L12 at position 5 are in accordance with  $\ln(x)$ , while that of only L8 and L12 at position 4 are in accordance with  $\ln(x)$ , which also supports the above conclusions. However, as it is impossible to accurately determine the specific location because of limited measurement positions, the data fitting method is used to determine the approximate location of the equilibrium point. The equilibrium points of L4, L8, and L12 are observed at 4.17 m, 3.19 m, and 2.13 m, respectively, indicating that the equilibrium position moves forward with the increase of the number of leaves. This is because the distance for adjustment is related to the water-blocking area. The water-blocking area per plant of P4, P8, and P12 is 32.63, 54.46, and 66.06 cm<sup>2</sup>, respectively, and thus the larger the water-blocking area is, the smaller the distance will be.

In order to understand the effect of different leaf numbers on flow simply and clearly, the whole flow is divided into three sections: upstream of vegetation area, interior of vegetation area, and downstream of vegetation area. Position 1, 5, and 7 are selected as the research objects respectively.

In order to better understand the effect of leaf number on the flow structure, the influence coefficient  $r = (u_i - u_0)/u_0$  is introduced to quantify the influence of aquatic plants on the flow structure, where  $u_i$  is the mean velocity at each point of L4, L8, and L12 and  $u_0$  is the mean velocity at each point of P0. Figure 5 shows that the  $r$  value of L4, L8, and L12 at position 1 is small (0.031–0.037) and shows no significant difference, indicating that aquatic plants have little influence on flow upstream the vegetation area. However, all  $r$  values of L4, L8, and L12 at position 5 and 7 are large and follow the order of  $L12 > L8 > L4$ , indicating that aquatic plants have a substantial influence on the mean velocity in and downstream the vegetation area, and the higher the number of leaves, the greater the influence of aquatic plants on the flow. However, there is no significant difference between different leaves.

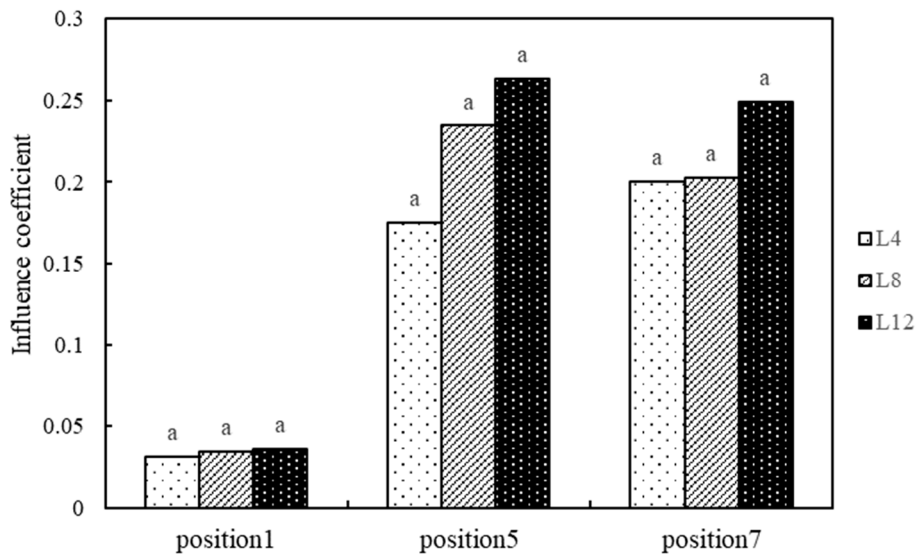


**Figure 5.** The influence coefficients at position 1, 5, and 7 (note: values within a position followed by the same letter are not significantly different (LSD,  $p < 0.05$ )).

### 3.2. Turbulence Structure

#### 3.2.1. Reynold’s Stress

The interaction between flow and aquatic plants can change flow momentum exchange, and the Reynold’s stress distribution under different leaf numbers is calculated, as shown in Figure 6.

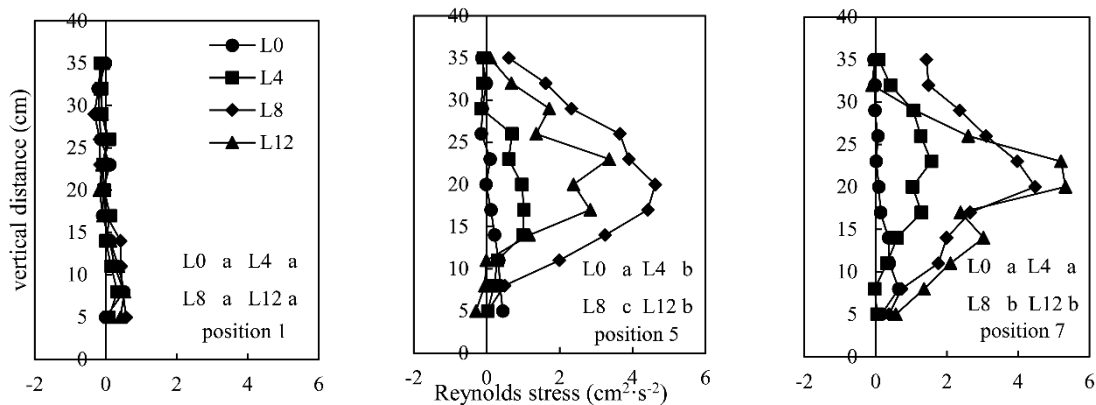


**Figure 6.** Reynold’s stress under different leaf numbers (note: values within a position followed by the same letter are not significantly different (LSD,  $p < 0.05$ )).

It can be seen from Figure 6 that the Reynold’s stress under L0, L4, L8, and L12 varies only slightly from −0.4 to 0.8 in the vertical direction at position 1 and there is no significant difference between them, indicating that aquatic plants have little effect on the Reynold’s stress upstream the vegetation area. At position 5, the Reynold’s stress in the vertical section changes little under L0; whereas that under L4, L8, and L12 increases until a maximum is reached near the top of the plant, and then decreases along the vertical direction. A similar phenomenon is observed in other studies [30,31]. There is a great difference in velocity at the top of the plant, resulting in the formation of a large number of vortices, and thus significant changes in the momentum exchange. It is also noted that flow can cause oscillation of aquatic plants, which is more pronounced near the top of the plant and produces more momentum exchange [18]. In addition, the number of leaves has a significant effect on Reynold’s stress in the vegetation area. With the increase of leaf number, the Reynold’s stress increases first and then decreases, indicating that the presence of a large number of leaves can inhibit momentum exchange in the vegetation area. Wilson et al. [14] also found that leaves inhibited momentum exchange. There may be two reasons for this: (1) the increase of leaf area will increase the momentum absorption area [14]; and (2) the increase of leaf volume will reduce plant oscillation. However, unlike the study of Wilson et al. [14], in which a large leaf (7 cm long and 10 cm wide) was used, a slender leaf (17 cm long and 0.05–1 cm wide) was used in this study to more accurately determine the relationship between flow momentum exchange and leaf area and leaf number. At position 7, the maximum Reynold’s stress increases with the increase of the number of leaves, indicating that the number of leaves has a significant effect on the Reynold’s stress downstream the vegetation area.

### 3.2.2. Quadrant Analysis

Coherent structures play an important role in mass and momentum exchange, and quadrant analysis is performed to identify these structures. In quadrant analysis, Reynold’s stress has different contributions according to the sign of instantaneous velocity fluctuation:

- Q1: Quadrant 1,  $u' > 0, v' > 0$ , outward interaction
- Q2: Quadrant 2,  $u' < 0, v' > 0$ , ejection
- Q3: Quadrant 3,  $u' < 0, v' < 0$ , inward interaction
- Q4: Quadrant 4,  $u' > 0, v' < 0$ , sweep

The average shear stress for the  $i$ th quadrant is

$$\overline{u'v'}_i = \frac{1}{n} \sum_{j=1}^{n_i} (u'v'_j)_i \tag{13}$$

where  $n_i$  is the number of events in the  $i$ th quadrant and  $j$  is the current sample number.

The data can be limited by a fixed amplitude threshold  $HT$  [32], where  $H$  is a threshold with the magnitude of unity, and  $T$  is usually defined as follows:

$$T = u'_{rms} v'_{rms} \tag{14}$$

$$|u'v'| > HT. \tag{15}$$

The concentration of the  $i$ th quadrant for a fixed threshold level can also be defined as follows:

$$C_H^i = \frac{1}{n} \sum_{j=1}^n x_{H,j}^i \tag{16}$$

where

$$x_{H,j}^i = \begin{cases} 1 & \text{if } |u'v'|_j > HT \text{ and belongs to the } i \text{ quadrant} \\ 0 & \text{otherwise} \end{cases} \tag{17}$$

The time-averaged Reynold’s stress for the  $i$ th quadrant can be expressed as follows:

$$S_{i,H} = \frac{1}{n} \sum_{j=1}^n (u'v')_j x_{H,j}^i \tag{18}$$

The Reynold’s stress contribution values are shown in Figure 7 and significance analysis of Reynold’s stress contribution values are shown in Table 3.

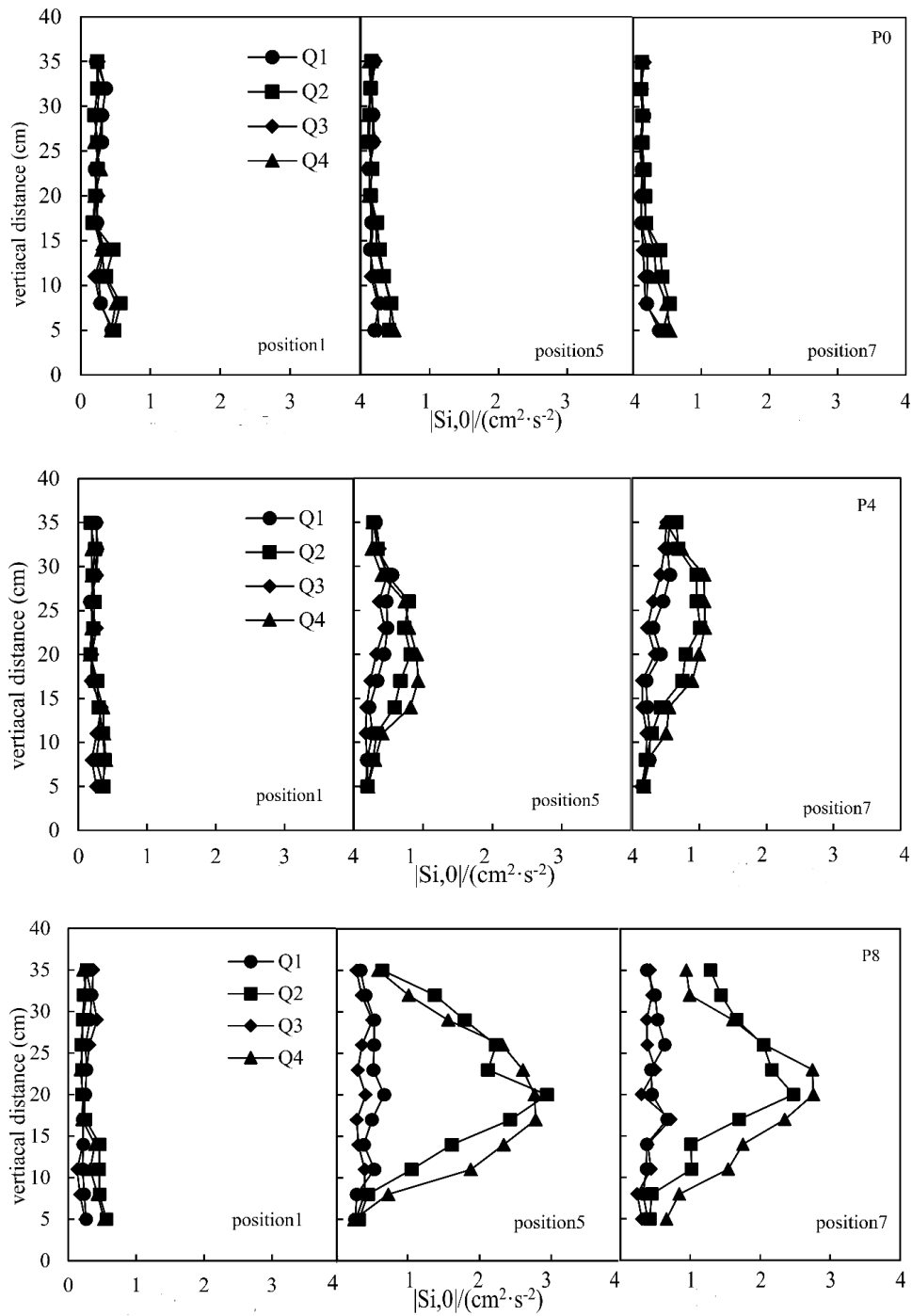


Figure 7. Cont.

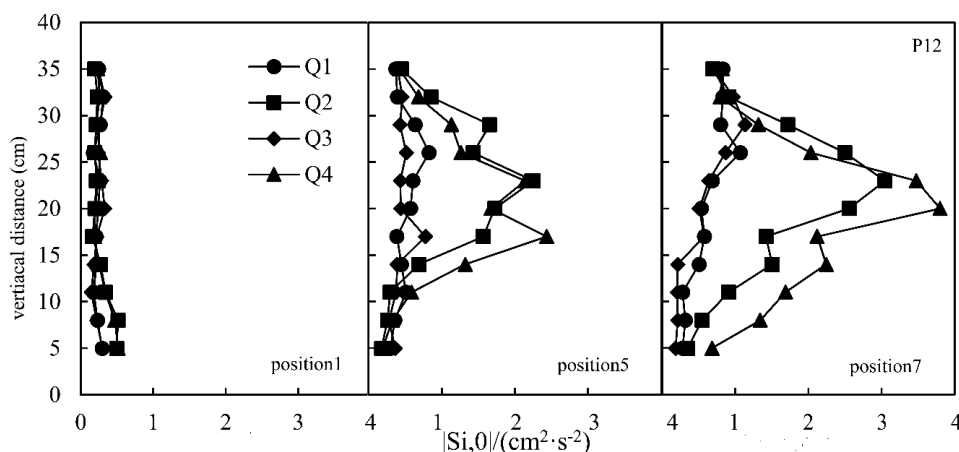


Figure 7. Reynold’s stress contribution values of the four quadrants.

It can be seen from Figure 7 that the Reynold’s stress contribution values under L0, L4, L8, and L12 are similar at position 1. There is no significant difference in the Reynold’s stress contribution values in the upper layer ( $z > 17$  cm), and the ejection and sweep of flow dominate in the lower layer ( $z < 17$  cm). At position 5, the contribution values under L4, L8, and L12 are increased significantly in all four quadrants, especially the values of Q2 and Q4. Thus, aquatic plants increase the momentum exchange in the vegetation area mainly by increasing the ejection and sweep. The contribution values in Q2 and Q4 reach a maximum near the top of the plant and then decrease to both sides, while those in Q1 and Q3 show no significant change. Ejection outweighs sweep in the upper free water layer and the opposite is true in the lower aquatic plant layer, which is similar to other studies [33]. In the four cases, the highest values are obtained in Q2 and Q4 under L8, indicating that the ejection and sweep are the strongest in the case of L8 in the vegetation area. At position 7, the contribution values in Q2 and Q4 also reach a maximum near the top of the plant and then decrease to both sides, while those in Q1 and Q3 also show no significant change. The values in Q2 and Q4 under L8 and L12 are significantly higher than those under L0, and the largest values of Q2 and Q4 are observed in L12. Thus, the momentum exchange downstream the vegetation area depends mainly on the ejection and sweep, and the higher the number of leaves, the higher the intensity of the ejection and sweep downstream the vegetation area.

Table 3. Significance analysis of Reynold’s stress contribution values.

Cases	Position											
	Position 1				Position 5				Position 7			
	Q1	Q2	Q3	Q4	Q1	Q2	Q3	Q4	Q1	Q2	Q3	Q4
L0	a	a	a	a	a	a	a	a	a	a	a	a
L4	ab	a	a	a	b	a	b	a	b	a	ab	a
L8	ab	a	a	a	c	b	b	b	b	b	bc	b
L12	b	a	a	a	c	c	c	c	c	b	c	b

Note: values within a column followed by the same letter are not significantly different (LSD,  $p < 0.05$ ).

### 3.2.3. Turbulent Kinetic Energy

Turbulent kinetic energy is an important indicator of the turbulence mixing ability, which is mainly determined by the change of instantaneous velocity. The turbulent kinetic energies under L0, L4, L8, and L12 are shown in Figure 8.

There is no significant difference in the turbulent kinetic energy at position 1, and the turbulent kinetic energy at the bottom is slightly larger than that in the upper layer, which indicates that aquatic plants have little influence on the turbulent kinetic energy upstream the vegetation area. However,

there is a significant difference between L0, L4, L8, and L12 in the vegetation area. The turbulent kinetic energy of L0 at position 5 is similar to that at position 1, and it is also slightly higher at the bottom than that in the upper layer. The turbulent kinetic energy of P4, P8, and P12 at position 5 increases gradually in the vertical direction and reaches a maximum near the top of the plant, and then decreases gradually. The turbulent kinetic energy of L8 is the largest, and it increases first and then decreases with the increase of the number of leaves. At position 7, the turbulent kinetic energy increases with the increase of the number of leaves, indicating that the number of leaves has a significant effect on the turbulent kinetic energy downstream the vegetation area.

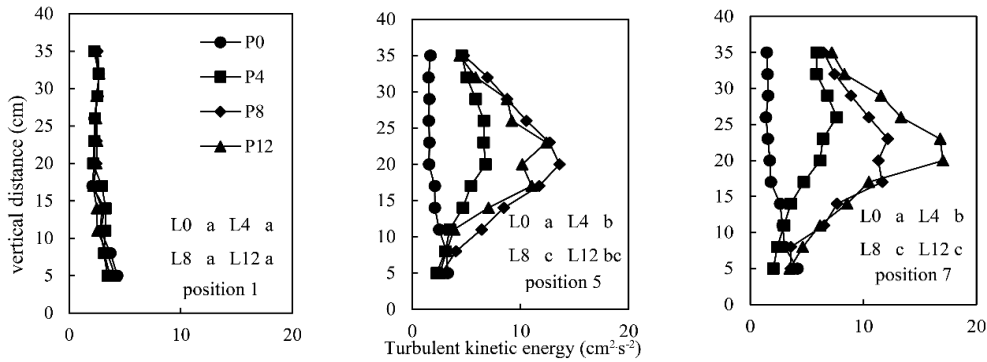


**Figure 8.** Turbulent kinetic energy under L0, L4, L8, and L12 (note: values within a position followed by the same letter are not significantly different (LSD,  $p < 0.05$ )).

### 3.3. Manning’s Roughness Coefficient

The Manning’s roughness coefficient reflects the flow resistance of a river channel, and is an indispensable parameter in river flow modelling. In this experiment, the Manning’s roughness coefficient of the non-vegetation flume is 0.0107, which is consistent with other studies [34]. The relationship between the Manning’s roughness coefficient and leaf number is shown in Figure 9. It shows that the Manning’s roughness coefficient reaches a maximum of 0.0238 under L12 and a minimum of 0.0196 under L4, and it increases linearly with the increase of the number of leaves. This is because the increase of the number of leaves can increase not only the water-blocking area of plants, but also the stiffness of plants. Li et al. [25] showed that the increase of plant density would reduce the flexibility of the vegetation area, resulting in a decrease in the curvature of plants and an increase in the Manning’s roughness coefficient. In a similar manner, increasing the number of leaves can also reduce the flexibility of individual plants.

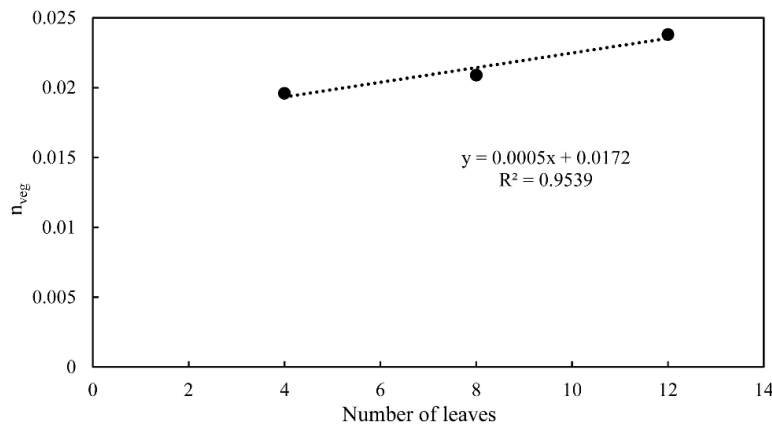


**Figure 9.** Relationship between the Manning’s roughness coefficient and the number of leaves.

#### 4. Conclusions

This study investigates the variation in flow characteristics with the number of leaves in an open-channel flume using ADV, and some important conclusions can be drawn from this study:

(1) The mean streamwise velocity profile in the upper layer obeys the logarithmic distribution law, and the velocity gradient increases with the increasing number of leaves. In the lower vegetation area, the mean flow velocity in the vertical direction decreases first and then increases, and the mean flow velocity of L4, L8, and L12 is 20.60%, 23.46%, and 29.53% lower than that of L0, respectively. The streamwise velocity reaches equilibrium at 4.17 m, 3.19 m, and 2.13 m under L4, L8, and L12, respectively, indicating that the higher the number of leaves, the further the equilibrium position. Aquatic plants have little influence on the mean flow velocity upstream the vegetation area, but a great influence in and downstream the vegetation area.

(2) Aquatic plants have little influence on the Reynold's stress and turbulent kinetic energy upstream the vegetation area. Aquatic plants increase the momentum exchange in the vegetation area mainly by increasing ejection and sweep, and the Reynold's stress and turbulent kinetic energy reach a maximum near the top of the plant and then decrease to both sides. Ejection and sweep still play a dominant role in momentum exchange in the vegetation area. With the increase of the number of leaves, Reynold's stress, contribution value of Q2 and Q4, and turbulent kinetic energy increase first and then decrease in the vegetation area. This is because the aquatic plant will induce momentum exchange, but the increase of the number of leaves would result in an increase in the momentum absorption area and reduce plant oscillation. Aquatic plants also have a significant effect on the Reynold's stress and turbulent kinetic energy downstream the vegetation area. Ejection and sweep still play a dominant role in momentum exchange, but Reynold's stress and turbulent kinetic energy increase with the increase of the number of leaves.

(3) The Manning's roughness coefficient reaches a maximum of 0.0238 under L12 and a minimum of 0.0196 under L4, and it increases linearly with the increase of the number of leaves.

This experiment provides some insights into the interactions between aquatic plants with different numbers of leaves and flow, which can be helpful for establishing river flow velocity models with complex aquatic plants.

**Author Contributions:** Conceptualization, P.Y., Y.T., X.L., and Q.F.; Formal analysis, P.Y. and J.L.; Methodology, T.L.; Writing—original draft, P.Y.; Writing—review & editing, Y.T.

**Funding:** This research was funded by the National Key R&D Program of China (2018YFC0406903) and the National Science Foundation of China (51609258, 51779268 and 51879273).

**Conflicts of Interest:** There is no conflict of interest in this manuscript.

#### References

- Chen, S.C.; Kuo, Y.M.; Li, Y.H. Flow characteristics within different configurations of submerged flexible vegetation. *J. Hydrol.* **2011**, *398*, 124–134. [[CrossRef](#)]
- Yilmazer, D.; Ozan, A.; Cihan, K. Flow Characteristics in the Wake Region of a Finite-Length Vegetation Patch in a Partly Vegetated Channel. *Water* **2018**, *10*, 459. [[CrossRef](#)]
- Huai, W.X.; Zhang, J.; Wang, W.J.; Katul, G.G. Turbulence structure in open channel flow with partially covered artificial emergent vegetation. *J. Hydrol.* **2019**, *573*, 180–193. [[CrossRef](#)]
- Wang, W.J.; Peng, W.Q.; Huai, W.X.; Katul, G.; Liu, X.B.; Dong, F.; Qu, X.D.; Zhang, H.P. Derivation of Canopy Resistance in Turbulent Flow from First-Order Closure Models. *Water* **2018**, *10*, 1782. [[CrossRef](#)]
- Lu, J.; Dai, H.C. Effect of submerged vegetation on solute transport in an open channel using large eddy simulation. *Adv. Water Resour.* **2016**, *97*, 87–99. [[CrossRef](#)]
- Longo, S. The effects of air bubbles on ultrasound velocity measurements. *Exp. Fluids* **2006**, *41*, 593–602. [[CrossRef](#)]
- Thomas, R.E.; McLelland, S.J. The impact of macroalgae on mean and turbulent flow fields. *J. Hydrodyn.* **2015**, *27*, 427–435. [[CrossRef](#)]

8. Wang, Y.; Zhang, H.; Yang, P.; Wang, Y. Experimental Study of Overland Flow through Rigid Emergent Vegetation with Different Densities and Location Arrangements. *Water* **2018**, *10*, 1638. [[CrossRef](#)]
9. Anjum, N.; Ghani, U.; Ahmed Pasha, G.; Latif, A.; Sultan, T.; Ali, S. To Investigate the Flow Structure of Discontinuous Vegetation Patches of Two Vertically Different Layers in an Open Channel. *Water* **2018**, *10*, 75. [[CrossRef](#)]
10. Zhang, H.Y.; Wang, Z.Y.; Xu, W.G.; Dai, L.M. Effects of Rigid Unsubmerged Vegetation on Flow Field Structure and Turbulent Kinetic Energy of Gradually Varied Flow. *River Res. Appl.* **2015**, *31*, 1166–1175. [[CrossRef](#)]
11. Huai, W.; Wang, W.; Hu, Y.; Zeng, Y.; Yang, Z. Analytical model of the mean velocity distribution in an open channel with double-layered rigid vegetation. *Adv. Water Resour.* **2014**, *69*, 106–113. [[CrossRef](#)]
12. Han, L.; Zeng, Y.; Chen, L.; Li, M. Modeling streamwise velocity and boundary shear stress of vegetation-covered flow. *Ecol. Indic.* **2018**, *92*, 379–387. [[CrossRef](#)]
13. Tang, H.; Tian, Z.; Yan, J.; Yuan, S. Determining drag coefficients and their application in modelling of turbulent flow with submerged vegetation. *Adv. Water Resour.* **2014**, *69*, 134–145. [[CrossRef](#)]
14. Wilson, C.; Stoesser, T.; Bates, P.D.; Batemann Pinzen, A. Open channel flow through different forms of submerged flexible vegetation. *J. Hydraul. Eng.* **2003**, *129*, 847–853. [[CrossRef](#)]
15. Li, J.; Yang, J.; Luo, J.; Cheng, H.; Bai, S. Influence of Growth of Flexible Submerged Plants on Turbulence Characteristics of Sediment-laden Flow. *Wetl. Sci.* **2012**, *04*, 446–450. [[CrossRef](#)]
16. Doods, W.; Biggs, B. Water velocity attenuation by stream periphyton and macrophytes in relation to growth form and architecture. *N. Am. Benthol. Soc.* **2002**, *21*, 2–15. [[CrossRef](#)]
17. Tong, X.; Liu, X.; Yang, T.; Hua, Z.; Wang, Z.; Liu, J.; Li, R. Hydraulic Features of Flow Through Local Non-Submerged Rigid Vegetation in the Y-shaped Confluence Channel. *Water* **2019**, *11*, 146. [[CrossRef](#)]
18. Devi, T.B.; Kumar, B. Turbulent flow statistics of vegetative channel with seepage. *J. Appl. Geophys.* **2015**, *123*, 267–276. [[CrossRef](#)]
19. Banerjee, T.; Muste, M.; Katul, G. Flume experiments on wind induced flow in static water bodies in the presence of protruding vegetation. *Adv. Water Resour.* **2015**, *76*, 11–28. [[CrossRef](#)]
20. Wang, W.-J.; Huai, W.-X.; Thompson, S.; Peng, W.-Q.; Katul, G.G. Drag coefficient estimation using flume experiments in shallow non-uniform water flow within emergent vegetation during rainfall. *Ecol. Indic.* **2018**, *92*, 367–378. [[CrossRef](#)]
21. Wu, D.; Ling, H.; Huang, Y. The Effect of Hydrodynamic Conditions on Growth Characteristics of *Vallisneria natans* and *Acorus calamus*. *Anhui Agric. Sci. Bull.* **2018**, *24*, 115–119. [[CrossRef](#)]
22. Zhang, Y.; Lai, X. Impact of *Vallisneria natans* on flow structure. *Adv. Water Sci.* **2015**, *26*, 99–106. [[CrossRef](#)]
23. Huai, W.; Wang, W.; Zeng, Y. Two-layer model for open channel flow with submerged flexible vegetation. *J. Hydraul. Res.* **2013**, *51*, 708–718. [[CrossRef](#)]
24. Huai, W.X.; Zeng, Y.H.; Xu, Z.G.; Yang, Z.H. Three-layer model for vertical velocity distribution in open channel flow with submerged rigid vegetation. *Adv. Water Resour.* **2009**, *32*, 487–492. [[CrossRef](#)]
25. Li, Y.; Wang, Y.; Anim, D.O.; Tang, C.; Du, W.; Ni, L.; Yu, Z.; Acharya, K. Flow characteristics in different densities of submerged flexible vegetation from an open-channel flume study of artificial plants. *Geomorphology* **2014**, *204*, 314–324. [[CrossRef](#)]
26. Noarayanan, L.; Murali, K.; Sundar, V. Manning's 'n' for staggered flexible emergent vegetation. *J. Earthq. Tsunami* **2013**, *7*, 1–18. [[CrossRef](#)]
27. Longo, S.; Di Federico, V.; Archetti, R.; Chiapponi, L.; Ciriello, V.; Ungarish, M. On the axisymmetric spreading of non-Newtonian power-law gravity currents of time-dependent volume: An experimental and theoretical investigation focused on the inference of rheological parameters. *J. Non-Newton. Fluid Mech.* **2013**, *201*, 69–79. [[CrossRef](#)]
28. Di Federico, V.; Longo, S.; King, S.E.; Chiapponi, L.; Petrolo, D.; Ciriello, V. Gravity-driven flow of Herschel–Bulkley fluid in a fracture and in a 2D porous medium. *J. Fluid Mech.* **2017**, *821*, 59–84. [[CrossRef](#)]
29. Luo, Y.; Zhang, S.; He, D.; Li, H. Uncertainty analysis of two kinds of parameters of hydraulic model tests. *Adv. Sci. Technol. Water Resour.* **2011**, *31*, 20–22. [[CrossRef](#)]
30. Devi, T.B.; Kumar, B. Flow characteristics in an alluvial channel covered partially with submerged vegetation. *Ecol. Eng.* **2016**, *94*, 478–492. [[CrossRef](#)]
31. Zhao, F.; Huai, W. Hydrodynamics of discontinuous rigid submerged vegetation patches in open-channel flow. *J. Hydro-Environ. Res.* **2016**, *12*, 148–160. [[CrossRef](#)]

32. Longo, S.; Losada, M.A. Turbulent structure of air flow over wind-induced gravity waves. *Exp. Fluids* **2012**, *53*, 369–390. [[CrossRef](#)]
33. Ghisalberti, M.; Nepf, H. The Structure of the Shear Layer in Flows over Rigid and Flexible Canopies. *Environ. Fluid Mech.* **2006**, *6*, 277–301. [[CrossRef](#)]
34. Xiang, S.; Wu, Y.; Bai, Y.; Mu, X. Experimental research on Manning' s roughness coefficient of an open channel with aquatic vegetation. *J. Hydraul. Eng.* **2017**, *48*, 874–881. [[CrossRef](#)]



© 2019 by the authors. Licensee MDPI, Basel, Switzerland. This article is an open access article distributed under the terms and conditions of the Creative Commons Attribution (CC BY) license (<http://creativecommons.org/licenses/by/4.0/>).